Journal of Cellular Biochemistry 95:817–826 (2005)

Investigating the Neuroprotective Mechanism of Action of a CDK5 Inhibitor by Phosphoproteome Analysis

Frank Gillardon,[1]* André Schrattenholz,[2] and Bernd Sommer[1]

[1]Boehringer Ingelheim Pharma GmbH & Co. KG, CNS Research, 88397 Biberach an der Riss, Germany
[2]ProteoSys AG, 55129 Mainz, Germany

Abstract Small molecule inhibitors of cyclin-dependent kinase 5 (CDK5) protect neurons from cell death following various insults. To elucidate the cellular mechanism of action we investigated changes in protein phosphorylation in cultured rat cerebellar granule neurons after administration of the CDK5 inhibitor Indolinone A. By immunoblot analysis we detected enhanced phosphorylation of the extracellular signal-regulated kinase1/2 (ERK1/2) and the Jun N-terminal kinase (JNK) substrate c-Jun. Co-administration of U0126, an inhibitor of ERK1/2, or SP600125, an inhibitor of JNK, blocked phosphorylation of ERK1/2 or c-Jun, but did not affect neuroprotection by the CDK5 inhibitor. By metal affinity chromatography, two-dimensional (2D) gel electrophoresis, and MALDI-TOF mass spectrometry we identified several phosphoproteins that accumulated in neurons treated with Indolinone A. Among them were proteins involved in neurotransmitter release, which is consistent with a physiological function of CDK5 in synaptic signaling. Moreover, we identified proteins acting in energy metabolism, protein folding, and oxidative stress response. Similar findings have been reported in yeast following inhibition of Pho85 kinase, which is homologous to mammalian CDK5 and acts in environmental stress signaling. These results suggest that inhibition of CDK5 activates stress responsive proteins that may protect neurons against subsequent injurious stimuli. J. Cell. Biochem. 95: 817–826, 2005.

Key words: neuroprotection; cyclin-dependent kinase; phosphorylation; two-dimensional gel electrophoresis; stress response

Cyclin-dependent kinases (CDKs) regulate cell cycle progression in proliferating cells. In differentiated neurons, the expression of mitotic CDKs is down-regulated, while CDK5 expression becomes up-regulated [Nguyen et al., 2002]. CDK5 knockout mice exhibit widespread disruption in neocortical layering indicating a role for Cdk5 in the development of the central nervous system. Reduction of CDK5 activity in cultured neurons points to a physiological function in cytoskeletal organization and synaptic transmission [Dhavan and Tsai, 2001].

Deregulation of CDK5 activity has been detected in the central nervous system of both Alzheimer's disease patients and mouse models of amyotrophic lateral sclerosis and Parkinson's disease. Moreover, administration of CDK inhibitors (e.g., roscovitine, flavopiridol) and expression of dominant-negative kinase mutants prevent neuronal cell loss in these models demonstrating that CDKs contribute to neurodegeneration [Dhavan and Tsai, 2001; Nguyen et al., 2002; Smith et al., 2003; Shelton and Johnson, 2004]. Using various CDK inhibitors, that originally were developed as anti-tumor agents, we have recently demonstrated that neuroprotective effectiveness correlates with inhibition of CDK5, but not mitotic CDKs [Weishaupt et al., 2003].

Deregulation of CDK5 results from proteolytic cleavage of its activatory subunit p35 to p25. CDK5/p25 translocates from the plasma membrane to the cytosol and nucleus, where novel substrates become hyperphosphorylated leading to neuronal cell death [Dhavan and Tsai, 2001; Nguyen et al., 2002]. Toxic substrates such as tau and neurofilament proteins have already been identified in Alzheimer's disease and amyotrophic lateral sclerosis. However, hyperphosphorylated tau and neurofilament

*Correspondence to: Dr. Frank Gillardon, Boehringer Ingelheim Pharma GmbH & Co. KG, CNS Research, Birkendorfer Str. 65, 88397 Biberach an der Riss, Germany.
E-mail: Frank.Gillardon@bc.boehringer-ingelheim.com

Received 15 September 2004; Accepted 24 January 2005
DOI 10.1002/jcb.20463

proteins could not be detected in other models of neurodegeneration, and thus, novel pathogenic substrates remain to be identified. Furthermore, since 518 putative protein kinase genes have recently been described in the human genome [Manning et al., 2002], it cannot be excluded that additional kinases may be inhibited by neuroprotective CDK5 inhibitors.

In order to get an overview on neuronal signal transduction cascades that are modulated by CDK5 inhibitors, we analyzed global changes in protein phosphorylation using two-dimensional (2D) gel electrophoresis and mass spectrometry [Mann et al., 2002]. Additionally, we performed immunoblot analysis using phospho-specific antibodies.

MATERIALS AND METHODS

Neuronal Cell Culture

Cerebellar granule neurons were isolated from 7-days old Wistar rat pups and were purified by density sedimentation. Briefly, cerebella were removed and dissociated with 1% trypsin/0.05% DNase in Ca^{2+}- and Mg^{2+}-free Hanks-balanced-salt-solution (Gibco, Karlsruhe, Germany) for 15 min at room temperature. After two washing steps with Hanks-balanced-salt-solution, 0.5% DNase was added and the cerebella were dissociated by trituration using Pasteur pipettes. Cerebellar granule neurons were subsequently separated by centrifugation at $1300 \times g$ for 15 min in a 40% (v/v) Percoll solution. The cells were harvested from the pellet and washed in ice-cold Minimum Essential Medium supplemented with 33 mM glucose (MEM; Gibco) followed by centrifugation for 5 min at $150 \times g$. Thereafter, cells were plated on poly-L-lysine-coated 96-well plates or Petri dishes ($2.5 \times 10^6/cm^2$) in MEM supplemented with 10% heat-inactivated fetal calf serum, 20 mM KCl, 100 U/ml penicillin, and 100 μg/ml streptomycin (Biochrom, Berlin, Germany). After 24 h in culture, the cells were treated with cytosine arabinoside (Sigma, Taufkirchen, Germany) in a final concentration of 5 μM. Cultures were maintained at 37°C, 5% CO_2 for 7 days without a change in medium. At day-in-vitro (DIV) seven cells were washed and culture medium was changed to serum-free MEM plus 20 mM KCl. Glutathione depletion was induced in cerebellar granule neurons by treatment with L-buthionine-sulfoximine (0.5 mM; Sigma), an inhibitor of glutamylcysteine synthetase [Wüllner et al., 1999]. The following commercially available kinase inhibitors were used: U0126 (10 μM; Upstate Biotechnology, Charlottesville, NC), an inhibitor of the extracellular signal-regulated kinase1/2 (ERK1/2)-activating kinase MAPK/ERK kinase1/2 (MEK1/2) [Favata et al., 1998], SP600125 (30 μM; Calbiochem, Bad Soden, Germany), an inhibitor of Jun N-terminal kinase (JNK) [Bennett et al., 2001], and roscovitine (30 μM; Calbiochem), an inhibitor of CDK4/5 [Walker, 1998; Bain et al., 2003]. Our CDK5 inhibitor Indolinone A has been tested against a panel of kinases in cell-free assays [Bain et al., 2003]. This compound inhibits CDK5 activity with an IC50 of 5 nM, whereas other cell death-promoting kinases, such as CDK1/2, JNK, p38 mitogen-activated protein kinase (p38MAPK), are not significantly blocked up to 1 μM [Weishaupt et al., 2003]. All kinase inhibitors were tested at concentrations that have shown activity in other cell culture systems before [Stanciu et al., 2000; Bennett et al., 2001; Crossthwaite et al., 2002; Weishaupt et al., 2003]. Compounds were administered in serum-free MEM at DIV 7, when expression of CDK1, CDK2, and CDK4 in cerebellar granule neurons is down-regulated, whereas expression of CDK5 is up-regulated [Courtney and Coffey, 1999].

Assessment of Cell Viability

Mitochondrial metabolic activity was tested using the Alamar Blue Assay (Serotec, Düsseldorf, Germany). The assay uses an indicator compound that changes from the oxidized, non-fluorescent to the reduced, fluorescent form in response to chemical reduction of the medium resulting primarily from mitochondrial succinate dehydrogenase activity. Alamar Blue solution was added to the medium at a final concentration of 5%. Cerebellar granule neurons were incubated for 2 h, thereafter fluorescence was monitored at 530 nm excitation and 590 nm emission wavelength in a Millipore CytoFluor Reader 2350 (Millipore, Eschborn, Germany).

Immunocytochemistry

For double immunofluorescent labeling, cerebellar granule neurons were cultured on Lab-Tek Chambered Coverglass. Following treatment neurons were fixed in phosphate-buffered saline (PBS) containing 4% paraformaldehyde for 40 min at 4°C. Cells were permeabilized with

100% methanol for 10 min at −20°C, blocked with 10% normal goat serum for 60 min at room temperature, and subsequently incubated with rabbit anti-phospho c-Jun (Ser73) antibody (1:100; Cell Signaling, Frankfurt a.M., Germany) and mouse anti-MAP2 antibody (1:100; Sigma) overnight at 4°C. Primary antibody was omitted as negative control. Biotinylated anti-rabbit immunoglobulin G, streptavidin-conjugated Alexa Fluor, and Cy3-conjugated anti-mouse immunoglobulin G, respectively, were used for detection. Immunofluorescence was visualized using a confocal laser scan microscope (Leica TCS; Leica, Bensheim, Germany).

Immunoblot Analysis

Neuronal cell cultures were washed twice with ice-cold PBS, rapidly scraped in ice-cold lysis buffer (62.5 mM Tris-HCl, pH 6.8, 2% sodium dodecyl sulfate, 50 mM dithiothreitol, 5% glycerol), and sonicated for 1 min. Cell lysates were centrifuged at 15,000 × g for 15 min and supernatants were loaded (15 μg/lane) on 12% sodium dodecyl sulfate-polyacrylamide minigels. Proteins were transferred to nitrocellulose membranes using a wet transfer system (Biorad, München, Germany). After blocking in buffer containing 20 mM Tris-HCl, pH 7.4, 500 mM NaCl, 0.05% Tween 20, and 5% bovine serum albumin for 90 min, the membranes were incubated overnight with the following primary antibodies: anti-phospho-p44/42 MAP kinase (ERK1/2), anti total p44/42 MAP kinase (ERK1/2), anti-phospho-c-Jun (Ser73), and anti total c-Jun (all at 1:1000; Cell Signaling). Horseradish peroxidase-conjugated secondary antibodies and enhanced chemiluminescence reagents (ECL; Amersham, Freiburg, Germany) were used for detection. Densitometric analysis of immunoblots was performed using the Versa Doc system and Quantity One software (Biorad).

Two-Dimensional Gel Electrophoresis and Mass Spectrometry

For 2D minigel electrophoresis and immunoblotting neurons were washed twice in ice-cold buffer (10 mM Tris-HCl, pH 7.0, 250 mM sorbitol), scraped directly in isoelectric focusing buffer (8M urea, 4% chaps, 20 mM Tris-HCl, pH 7.4, 1% dithiothreitol, phosphatase inhibitor cocktail, 0.8% IPG-buffer from Amersham) and sonicated. Cell lysates were centrifuged at 15,000 × g for 15 min and supernatants were diluted with isoelectric focusing buffer. Proteins were loaded on IPG strips (Immobiline DryStrip, pH 4–7, 7cm; Amersham) during rehydration and focused using an Ettan IPGphor and standard protocols (Amersham). Second dimension sodium dodecyl sulfate-polyacrylamide gel electrophoresis and immunoblotting was performed as described above. A polyclonal rabbit anti-glucose regulated protein 58 antibody (1:1000; Stressgen, Victoria, Canada) or a mouse monoclonal anti-phosphotyrosine antibody (clone PY69, 1:1000, Transduction Lab, Lexington, KY) was used for detection.

For large scale experiments cultured neurons (30 Petri dishes per experimental group) were rinsed twice with ice-cold PBS and then scraped in lysis buffer (50 mM Tris-HCl, pH 7.4, 6% lithium dodecylsulphate, 6% Triton-X-100, 5 mM sodium fluoride, 5 mM sodium glycerolphosphate, 1 mM sodium ortho-vanadate, 5 mM EDTA, Complete protease inhibitor cocktail). Subsequent analysis was performed at ProteoSys AG (Mainz, Germany) as has been described in detail elsewhere [Sommer et al., 2004; Wang et al., 2004]. Phosphoproteomes were isolated by Fe-agarose columns equilibrated with binding buffer (50 mM bis-(hydroxyethyl)-piperazine-HCl, pH 3.4, 2% Triton X-100) [Muszynska et al., 1986]. Samples equilibrated in binding buffer were loaded to the column and eluted with 50 mM NaH_2PO_4 in binding buffer. The trichlororacetic acid precipitate of the eluate was dissolved in isoelectric focusing buffer (7M urea, 1% Triton X-100, 10% glycerine, 2M thiourea, 4% chaps, 20 mM Tris-HCl, pH 7.4, 1% dithiothreitol, 0.8% IPG-buffer from Amersham). For total proteome analysis an aliquot of samples equilibrated in binding buffer was precipitated and dissolved in isoelectric focusing buffer. Two dimensional gel electrophoresis was performed as described previously [Soskic et al., 1999; Predic et al., 2002] and proteins were visualized by silver staining according to Shevchenko et al. [1996]. Gels were run in triplicate and were automatically matched according to a molecular weight scale and selected landmarks. The software used was Phoretix2D (Nonlinear Dynamics, Newcastle, UK) and Delta2D (Decodon, Greifswald, Germany). Comparison of aligned gels revealed differentially existing protein spots. Selected spots were excised from the gel by a picking robot (ProPick; Genomic Solutions, Ann Arbor, MI) and proteins in gel pieces were trypsin digested by a ProGest-robot (Genomic

Solutions). A ProMS-robot (Genomic Solutions) was used to apply samples for MALDI-TOF mass spectrometry onto an anchor target (Bruker, Bremen, Germany). Identification of selected protein spots was performed by peptide mass fingerprinting. Spectra were obtained using an Autoflex MALDI time-of-flight mass spectrometer (Bruker) in the reflector mode within a mass range from m/z 800 to 4000. The mass spectra obtained for the protein digests were calibrated and annotated automatically. The resulting peptide mass fingerprints were searched against the non-redundant NCBI Protein Sequence Database (version of May 2002) using Mascot Server software v. 1.8. (Matrix Science, London, UK).

Statistics

For each experimental group three neuronal cell cultures were used at minimum. All experiments were performed at least in duplicate producing similar results. Data are given as mean ± SD unless stated otherwise. Statistical analysis was performed using Student's *t*-test, and $P < 0.05$ was considered significant.

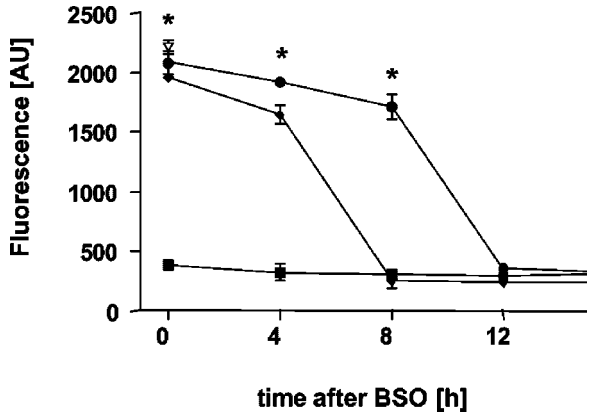

Fig. 1. CDK5 inhibitors prevent neuronal cell death when added after L-buthionine-sulfoximine. Cerebellar granule neurons were cultured in 96-well plates for 6 days. Neurons were then treated with the glutamylcysteine synthetase inhibitor, L-buthionine-sulfoximine (BSO) (0.5 mM). Roscovitine (30 μM, filled diamonds), Indolinone A (0.3 μM, filled circles), or vehicle (filled squares) was added at 0, 4, 8, or 12 h after BSO administration. Sham-treated control cultures are indicated by open diamond (0 h). After a total incubation of 24 h cell viability was tested by Alamar Blue assay. Data presented are the mean ± SD of triplicate determinations. Asterisks indicate a *P* value < 0.05 as determined by Student's *t*-test. Analogous results were obtained in three independent experiments.

RESULTS

Neuroprotection by CDK5 Inhibitors

Buthionine sulfoximine (BSO) treatment of primary neuronal cell cultures causes a slow decline of mitochondrial glutathione levels resulting in accumulation of reactive oxygen species, mitochondrial dysfunction, and delayed non-apoptotic cell death [Wüllner et al., 1999; Weishaupt et al., 2003]. We have recently demonstrated that co-administration of Indolinone A promotes survival of BSO-treated cerebellar granule neurons with an EC50 of 150 nM [Weishaupt et al., 2003]. In the present study, we first tested the neuroprotective efficacy of two CDK5 inhibitors (Indolinone A, roscovitine) when added at various time points after BSO. Cell viability was assessed following 24 h of BSO treatment by Alamar Blue assay. As can be seen from Figure 1, both compounds prevent cell death, when added within 4 h after BSO administration. Roscovitine (30 μM) was ineffective at 8 h after BSO, whereas neuroprotection by Indolinone A (0.3 μM) declined between 8 and 12 h (Fig. 1). Administration of BSO alone did not affect Alamar Blue reduction up to 16 h [Wüllner et al., 1999; Weishaupt et al., 2003]. These findings indicate that the neuroprotective mechanism(s) of action of CDK5 inhibitors are initiated within 4 h after compound administration and long before BSO-induced mitochondrial dysfunction becomes detectable. Subsequent studies that aimed at elucidating the mechanism(s) of action of Indolinone A, therefore, focused on changes in protein phosphorylation at early time points after compound treatment.

Effect of Indolinone A on Kinase Signaling Cascades

Activity of anti-apoptotic ERK versus pro-apoptotic JNK has been shown to determine neuronal survival [Xia et al., 1995] and studies in mutant mice lacking CDK5 activity point to a cross-talk between CDK5 and ERK/JNK signaling pathways [Li et al., 2002; Sharma et al., 2002]. Rat ERK1/2 is activated by phosphorylation at Thr183 and Tyr185 which can be detected by phospho-specific antibodies. As shown in Figure 2, incubation of rat cerebellar granule neurons with the CDK5 inhibitor Indolinone A (0.3 μM for 3 h) caused a 2.5-fold increase ($P < 0.05$, *t*-test) in the ratio of phospho-ERK1 to total ERK1 compared to sham-treated cultures. Active JNK phosphorylates transcription factor c-Jun at Ser63 and Ser73.

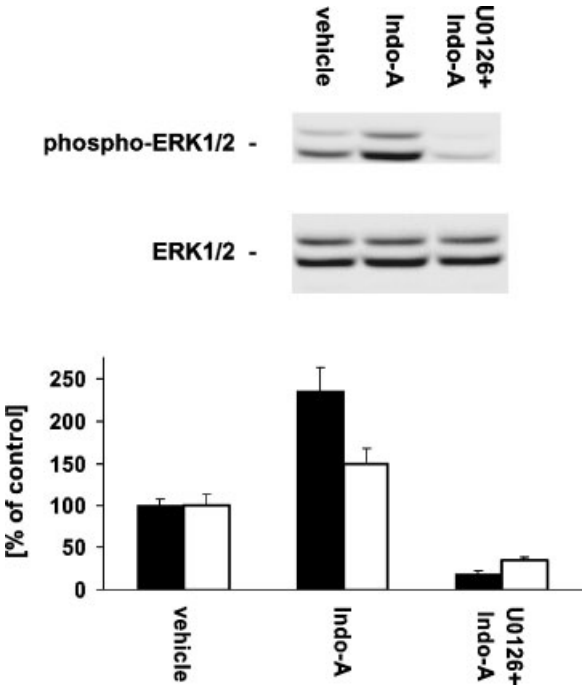

Fig. 2. The CDK5 inhibitor Indolinone A causes ERK phosphorylation/activation that can be prevented by U0126. Cerebellar granule neurons were cultured in 60-mm Petri dishes for 6 days. Neurons were then incubated in either Indolinone A (0.3 μM) or Indolinone A (0.3 μM) plus U0126 (10 μM) for 3 h. Active ERK1/2 or total ERK1/2 (also termed p44/p42 MAP kinase) was detected in protein lysates by immunoblot analysis using a phospho-ERK1/2 specific antibody or a total ERK1/2 antibody. Densitometric analysis of immunoblots showing the ratio of phospho-ERK1 to total ERK1 (filled bar) and phospho-ERK2 to total ERK2 (open bar), respectively, is depicted in the lower panel. Data presented are the mean ± SD of three independent experiments.

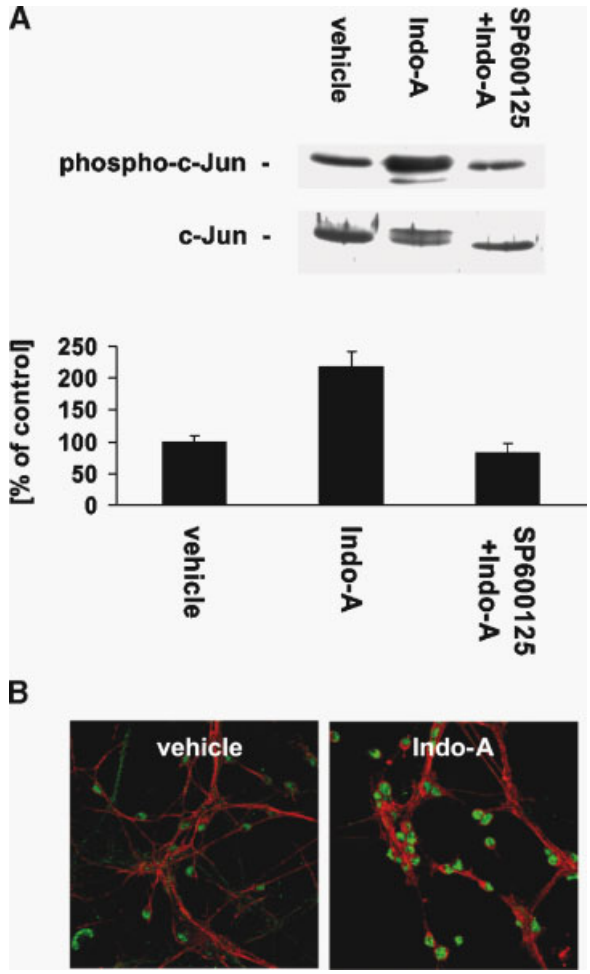

Fig. 3. Indolinone A induces activation of JNK that can be inhibited by SP600125. Cerebellar granule neurons were treated with either Indolinone A (0.3 μM) or Indolinone A (0.3 μM) plus SP600125 (30 μM) for 3 h. **A**: The JNK substrate phospho-c-Jun or total c-Jun protein was detected in protein lysates by immunoblot analysis using a phospho-c-Jun(Ser73) specific antibody or a total c-Jun antibody. A partial shift in the total c-Jun immunoreactive band is visible following Indolinone-A administration. Densitometric analysis showing the increase in phospho-Jun is depicted in the lower panel. Data presented are the mean ± SD of three independent experiments. **B**: Nuclear localization of phospho-c-Jun(Ser73) (green) in Indolinone A-treated neurons was assessed by immunocytochemistry. Cytoplasmic MAP2 immunofluorescence can be seen in red. [Color figure can be viewed in the online issue, which is available at www.interscience.wiley.com.]

Administration of 0.3 μM Indolinone A significantly ($P < 0.05$, t-test) increased c-Jun phosphorylation at Ser73 by about two fold after 3 h, as assessed by immunoblotting (Fig. 3A). In the same experimental group the total c-Jun immunoreactive band partially shifted, indicating phosphorylation of c-Jun at multiple sites. Phospho-c-Jun(Ser73) immunoreactivity localized to the nucleus of cerebellar granule neurons, as shown by immunocytochemistry in Figure 3B. The increase in phospho-ERK1 and phospho-c-Jun was maintained up to 9 h after compound treatment and was not detected following administration of BSO alone. In contrast, Indolinone A treatment did not affect phosphorylation of AKT at Thr308 or phosphorylation of p38 MAPK at Thr180/Tyr182 in cultured neurons (data not shown).

To assess whether activation of anti-apoptotic ERK by Indolinone A underlies its neuroprotective effectiveness, we co-incubated cerebellar granule neurons with Indolinone A and U0126, an inhibitor of the ERK-activating kinase MEK1/2 [Favata et al., 1998]. U0126 at 10 μM completely prevented the increase in ERK1/2 phosphorylation by Indolinone A without affecting total ERK1/2 levels (Fig. 2). Treatment with either U0126 (10 μM) or Indolinone A (0.3 μM) alone for 24 h did not alter cell viability as

assessed by Alamar Blue reduction (95.1% ± 3.7% and 103.6% ± 4.1%, respectively, of sham-treated control cultures). More importantly, co-administration of U0126 (10 μM) did not significantly affect neuroprotection by Indolinone A (0.3 μM) against BSO-induced cell death (82.6% ± 8.6% of control cultures). To elucidate the physiological relevance of Indolinone A-induced c-Jun phosphorylation, we incubated cerebellar granule neurons with the JNK inhibitor SP600125 [Bennett et al., 2001] plus Indolinone A. As shown by immunoblotting in Figure 3A, SP600125 (30 μM) completely blocked both the increase in phospho-c-Jun (Ser73) and the shift of the total c-Jun band in neuronal cultures treated with Indolinone A (0.3 μM, 3 h). SP600123 alone at 30 μM did not significantly change cell viability at 24 h (84.5% ± 3.6% of control cultures). Moreover, co-treatment with 30 μM SP600123 did not alter prevention of BSO-induced cell death by Indolinone A (90.7% ± 2.8% of control cultures).

Phosphoproteome Analysis

In order to identify proteins whose phosphorylation is modulated by Indolinone A treatment, phosphoproteins were enriched by metal affinity chromatography and proteins were separated by 2D gel electrophoresis. Representative silver-stained gels are shown in Figure 4. Protein spots were identified by MALDI-TOF mass spectrometry with Mascot scores ≥65. Only few spots showed differences in intensity following densitometric analysis of gel triplicates. Nine proteins exhibited a moderate increase in the phosphoprotein fraction 3 h after Indolinone A administration (Table I), whereas proteins showing a decline could not be detected. The proteins could be grouped according to their known function as follows: stress-inducible proteins and chaperones (heat shock cognate protein 70, turned on after division 64, chaperonin subunit ε, glucose regulated protein 58), proteins functioning in energy metabolism (creatine kinase-B, enolase α, isocitrate dehydrogenase α, lactate dehydrogenase-B), and proteins acting in neuronal signaling (vacuolar H^+-ATPase α).

By 2D minigel electrophoresis and immunoblotting using an anti-glucose regulated protein 58 antibody we detected two spots with the same molecular weight (about 60 kDa) but slightly different pI (Fig. 5A). Densitometric analysis revealed that the more acidic spot increased in intensity by approximately 70% after Indolinone A treatment, whereas intensity of the basic spot declined giving indirect evidence for an increase in phosphorylation of glucose regulated protein 58. Enhancement of tyrosine phosphorylation by Indolinone A was also observed on 2D immunoblots using an anti-phosphotyrosine antibody (Fig. 5B).

Finally, prediction of potential phosphorylation sites was performed using the computer

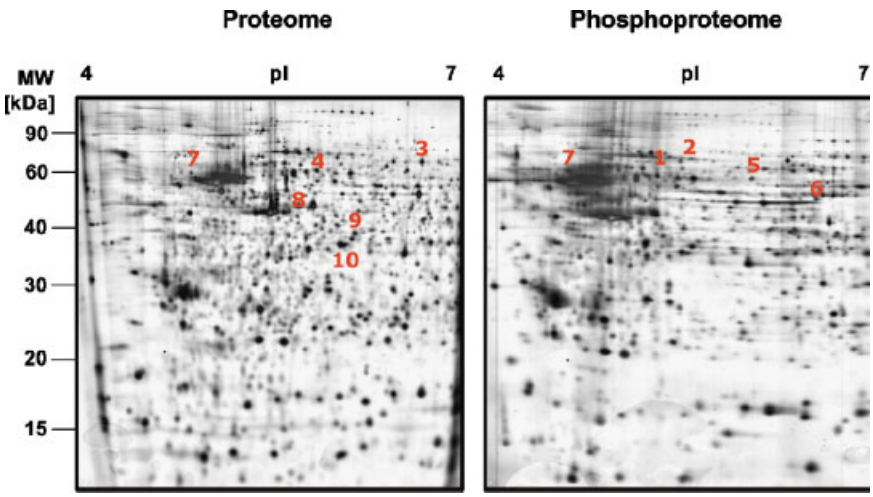

Fig. 4. Representative two-dimensional (2D) gel images visualized by silver staining. Protein extracts were prepared from cultured neurons 3 h after Indolinone A administration, and were separated by 2D gel electrophoresis (pI range from 4 to 7) (proteome). Alternatively, phosphoproteins were enriched by metal affinity chromatography before 2D gel electrophoresis (phosphoproteome). Numbered spots were identified by MALDI-TOF mass spectrometry after in-gel trypsin digestion. [Color figure can be viewed in the online issue, which is available at www.interscience.wiley.com.]

TABLE I. Proteins That Increase in the Phosphoprotein Fraction Following Administration of a CDK5 Inhibitor to Cultured Neurons

No.	Accession no.	Protein	Mascot score	MW [Da] Gel	MW [Da] DB	pI Gel	Change (%)
1	gi|13242237	(NM_024351) heat shock cognate protein 70	126	70,000	71,055	5.6	25 + 3
2	gi|6680752	(NM_007508) ATPase, H^+ transporting, lysosomal (vacuolar proton pump), alpha 70 kDa, isoform 1	236	75,000	68,567	5.7	23 + 8
3	gi|1351260	Dihydropyrimidinase related protein-2 (DRP-2) (turned on after division, 64 kDa protein) (TOAD-64)	102	66,000	62,638	6.4	34 + 13
4	gi|6671702	(NM_007637) chaperonin subunit 5 (epsilon)	85	59,000	60,042	5.8	51 + 10
5	gi|13994168	(NM_031580) glucose regulated protein, 58 kDa	206	61,000	57,044	6.2	86 + 10
6	gi|6978809	(NM_012554) enolase 1, alpha	126	48,000	47,428	6.4	54 + 5
7	gi|203476	(M57664) creatine kinase-B	78	46,000	40,883	5.7	19 + 7
8	gi|18250284	(NM_029573) isocitrate dehydrogenase 3 (NAD+) alpha	83	39,000	40,069	6.1	37 + 7
9	gi|6678674	(NM_008492) lactate dehydrogenase-B	126	37,000	36,834	6.0	32 + 8

MW, molecular weight; DB, database.

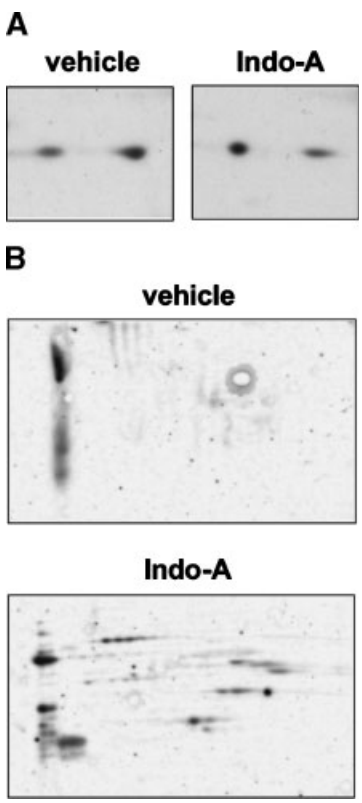

Fig. 5. **A**: Two-dimensional minigel electrophoresis and immunoblotting using an anti-glucose regulated protein 58 antibody. Cerebellar granule neurons were treated with Indolinone A (Indo-A, 0.3 μM) or vehicle for 3 h. A shift to the more acidic protein spot is visible following CDK5 inhibitor administration. The pH range from 6.0 to 6.4 is depicted. **B**: Two-dimensional minigel electrophoresis and immunoblotting using an anti-phosphotyrosine antibody. The number of phosphotyrosine immunoreactive protein spots increases after treatment with Indolinone A (Indo-A, 0.3 μM, 3 h). The pH range from 4.0 to 7.0 is depicted.

program NetPhos (www.cbs.dtu.dk/services/NetPhos) [Blom et al., 1999]. Phosphorylation at serine, threonine, or tyrosine residues was predicted with a score >0.9 for all proteins listed in Table I.

DISCUSSION

In several studies, blockade of CDK activity using either dominant-negative kinase mutants or small molecule inhibitors has been demonstrated to prevent neuronal cell death [Nguyen et al., 2002; Smith et al., 2003; Shelton and Johnson, 2004]. However, cellular signaling cascades and kinase substrates that are targeted by neuroprotective CDK inhibitors are poorly characterized. In our previous study, we have demonstrated that pharmacological inhibition of CDK5, but not mitotic CDKs, prevents both necrotic cell death induced by glutathione depletion and apoptotic cell death following serum deprivation [Weishaupt et al., 2003]. In the present study, we analyzed the signaling pathways that may either directly or indirectly be targeted by our CDK5 inhibitor. Since we observed that the neuroprotective mechanisms of action of Indolinone A are initiated within 4 h after administration, subsequent studies focused at early changes in protein phosphorylation in neuronal cell cultures.

In a simplistic view, neurotrophic factors signal via the ERK cascade supporting neuronal survival, whereas stress or injury activates the JNK pathway favouring neuronal death [Xia et al., 1995]. Surprisingly, our neuroprotective CDK5 inhibitor caused a rapid and sustained

activation of both anti-apoptotic ERK1/2 and pro-apoptotic JNK in cultured neurons. This is consistent with recent studies in mutant mice lacking either CDK5 or its activator p35, where elevated levels of phospho-c-Jun or phospho-ERK have been detected in brain extracts [Li et al., 2002; Sharma et al., 2002]. Thus, short-term pharmacological blockade of endogenous CDK5 by Indolinone A in neuronal cell cultures may result in disinhibition of JNK and MEK similar to *CDK5* gene knockout in mice.

Indolinone A-mediated JNK activation was blocked using the pan-JNK inhibitor SP600125 which exhibits 100-fold selectivity against recombinant ERK2 or p38 MAPK, and blocks c-Jun phosphorylation with an IC50 of 5–10 μM in cellular assays [Bennett et al., 2001]. Although SP600125 reduced c-Jun phosphorylation to basal levels in our study, the JNK inhibitor had no effect on Indolinone A-mediated neuroprotection against BSO-induced cell death. Thus, disinhibition of JNK appears to be irrelevant for the effects of CDK5 inhibitors, at least in our model. Alternatively, activation of JNK signaling may be overridden by the concommitant stimulation of survival-promoting ERK1/2. To test this possibility, we administered U0126, an inhibitor of the ERK-activating kinases MEK1/2, which displays >100-fold selectivity against JNK, p38 MAPK, MAPK kinases, CDK2, and CDK4 [Favata et al., 1998]. Indolinone A-induced ERK1/2 phosphorylation was completely blocked by U0126 co-treatment, however, neuroprotection by Indolinone A remained unchanged. The role of ERK in neurodegeneration following oxidative injury is controversial, and U0126 has been reported to either enhance or reduce neuronal survival during oxidative stress in vitro [Stanciu et al., 2000; Crossthwaite et al., 2002].

By metal affinity chromatography and 2D gel electrophoresis we detected a moderate increase in several phosphoproteins in Indolinone A-treated cell cultures. Accumulation together with the lack of a CDK5 phosphorylation consensus sequence (S/T)PX(K/H/R) [Dhavan and Tsai, 2001] is speaking against a role as CDK5 substrates. In cell-free assays, CDK5 has been shown to modulate the activity of various protein kinases (e.g., MEK1, JNK, p21-activated kinase, protein kinase A) and protein phosphatases (e.g., phospho-protein phosphatase 1) [Agarwal-Mawal and Paudel, 2001; Dhavan and Tsai, 2001], which might explain the complex changes in cellular protein phosphorylation observed in our study. Since proteins were extracted 3 h following compound treatment, changes are likely due to rapid post-translational modification rather than protein biosynthesis, as already indicated by the specific alterations in phosphorylation of ERK1/2, and c-Jun shown on 1D immunoblots. By 2D minigel electrophoresis and immunoblotting we detected a pI shift in glucose regulated protein 58, as has been shown following protein modification by phosphorylation using other kinase inhibitors [Lewis et al., 2000]. An increase in tyrosine-phosphorylated protein spots following Indolinone A administration was also demonstrated using an anti-phosphotyrosine antibody. Additionally, phosphorylation of dihydropyrimidinase related proteins was confirmed in a parallel study by MS/MS analysis [Sommer et al., 2004]. It should be mentioned however, that other methods for phosphoproteome analysis have been developed, which may show higher sensitivity and accuracy [Mann et al., 2002].

Nevertheless, our data provide novel insight into the role of CDK5 in neurotransmission and stress signaling. Synapsin 1, mammalian unc-18 homologue (MUNC-18), and amphiphysin have already been identified as presynaptic substrates of CDK5 that are involved in synaptic vesicle release and recycling [Dhavan and Tsai, 2001]. We detected an increase in phosphorylation of vacuolar H^+-ATPase α (V-ATPase) which generates the proton-motive force that is utilized for accumulation of neurotransmitters into synaptic vesicles [Nelson, 1993]. Although phosphorylation of V-ATPase may be indirectly affected by our CDK5 inhibitor, these findings substantiate the role of CDK5 in modulating synaptic function as has been shown by others [Samuels and Tsai, 2003; Tan et al., 2003].

Treatment with Indolinone A also lead to an increased phosphorylation of several proteins acting in energy metabolism, e.g., creatine kinase-B, enolase α, isocitrate dehydrogenase α, and lactate dehydrogenase-B. Brain-type creatine kinase-B catalyzes the reaction from phospho-creatine to ATP, and phosphorylation reduces the Km for phospho-creatine [Quest et al., 1990], which might contribute to the preservation of mitochondrial function in Indolinone A-treated cultures under stress

[Weishaupt et al., 2003]. Moreover, increased tyrosine-phosphorylation of creatine kinase, lactate dehydrogenase, glucose regulated protein 58, heat shock cognate protein 70, and chaperonin ε has recently been demonstrated by phosphoproteome analysis in cell lines, where phosphorylation is involved in heat shock signaling and thermotolerance [Kim et al., 2002]. Heat shock cognate protein 70, turned on after divison 64, and enolase γ have been detected in an oxidoreductase complex, which is involved in vesicle fusion and oxidative stress response [Bulliard et al., 1997]. Changes in phosphorylation following Indolinone A treatment further support a role for CDK5 in neurotransmission and stress signaling.

A novel function for CDK5 in stress signaling is also indicated by recent findings in yeast. Complementation studies have shown that mammalian CDK5/p35 is a functional homologue of yeast Pho85/Pho80 protein kinase [Huang et al., 1999], which is part of the phosphate-responsive signal transduction pathway (PHO system) [Carroll and O'Shea, 2002]. Similar to our data, chemical inhibition of Pho85 in the absence of stressful conditions causes the rapid activation of genes involved in a generic environmental stress response including proteins acting in energy metabolism, protein folding, oxidative stress response, and membrane fusion [Carroll et al., 2001]. Notably, this stress response was transient and only detectable after the rapid loss of Pho85 activity caused by chemical inhibition but not in *Pho85* gene-deficient yeast mutants. Thus, it may be speculated that our CDK5 inhibitor induces a similar response in cultured neurons leading to functional neuroprotection against stressful stimuli (e.g., glutathione depletion or serum/potassium deprivation) that causes delayed neuronal cell death [Weishaupt et al., 2003]. To show a causal relationship, expression of candidate neuroprotective proteins should be inhibited by siRNA technology. However, siRNA knockdown of a single candidate might be ineffective, if a battery of stress-responsive genes mediates neuroprotection. Finally, we cannot exclude that experimental inhibition of CDK5 might induce disturbances in cellular physiology that trigger a stress response. This response might then protect against a subsequent harmful stressor, a phenomenon known as preconditioning or cross-tolerance [Dirnagl et al., 2003].

ACKNOWLEDGMENTS

The authors thank C. Bentz, G. Schutzius, and E. Schmidt for excellent technical assistance. The authors declare that they have competing financial interests.

REFERENCES

Agarwal-Mawal A, Paudel HK. 2001. Neuronal Cdc2-like protein kinase (Cdk5/p25) is associated with protein phosphatase 1 and phosphorylates inhibitor-2. J Biol Chem 276:23712–23718.

Bain J, McLauchlan H, Elliott M, Cohen P. 2003. The specificities of protein kinase inhibitors: An update. Biochem J 371:199–204.

Bennett BL, Sasaki DT, Murray BW, O'Leary EC, Sakata ST, Xu W, Leisten JC, Motiwala A, Pierce S, Satoh Y, Bhagwat SS, Manning AM, Anderson DW. 2001. SP600125, an anthrapyrazolone inhibitor of Jun N-terminal kinase. Proc Natl Acad Sci USA 98:13681–13686.

Blom N, Gammeltoft S, Brunak S. 1999. Sequence and structure-based prediction of eukaryotic protein phosphorylation sites. J Mol Biol 294:1351–1362.

Bulliard C, Zurbriggen R, Tornare J, Faty M, Dastoor Z, Dreyer J-L. 1997. Purification of a dichlorophenol-indophenol oxidoreductase from rat and bovine synaptic membranes: Tight complex association of a glyceraldehyde-3-phosphate dehydrogenase isoform, TOAD64, enolase-γ and aldolase C. Biochem J 324:555–563.

Carroll AS, O'Shea EK. 2002. Pho85 and signaling environmental conditions. Trends Biochem Sci 27:87–93.

Carroll AS, Bishop AC, DeRisi JL, Shokat KM, O'Shea EK. 2001. Chemical inhibition of Pho85 cyclin-dependent kinase reveals a role in the environmental stress response. Proc Natl Acad Sci USA 98:12578–12583.

Courtney MJ, Coffey ET. 1999. The mechanism of Ara-C-induced apoptosis of differentiating cerebellar granule neurons. Eur J Neurosci 11:1073–1084.

Crossthwaite AJ, Hasan S, Williams RJ. 2002. Hydrogen peroxide-mediated phosphorylation of ERK1/2, Akt/PKB and JNK in cortical neurones: Dependence of Ca^{2+} and PI3-kinase. J Neurochem 80:24–35.

Dhavan R, Tsai L-H. 2001. A decade of CDK5. Nat Rev Mol Cell Biol 2:749–759.

Dirnagl U, Simon RP, Hallenbeck JM. 2003. Ischemic tolerance and endogenous neuroprotection. Trends Neurosci 26:248–254.

Favata MF, Horiuchi KY, Manos EJ, Daulerio AJ, Stradley DA, Feeser WS, Van Dyk DE, Pitts WJ, Earl RA, Hobbs F, Copeland RA, Magolda RL, Scherle PA, Trzaskos JM. 1998. Identification of a novel inhibitor of mitogen-activated protein kinase kinase. J Biol Chem 273:18623–18632.

Huang D, Patrick G, Moffat J, Tsai L-H, Andrews B. 1999. Mammalian Cdk5 is a functional homologue of the budding yeast Pho85 cyclin-dependent protein kinase. Proc Natl Acad Sci USA 96:14445–14450.

Kim H-J, Song EJ, Lee K-J. 2002. Proteomic analysis of protein phosphorylation in heat shock response and thermotolerance. J Biol Chem 277:23193–23207.

Lewis TS, Hunt JB, Aveline LD, Jonscher KR, Louie DF, Yeh JM, Nahreini TS, Resing KA, Ahn NG. 2000. Identification of novel MAP kinase pathway signaling targets by functional proteomics amd mass spectrometry. Mol Cell 6:1343–1354.

Li B-S, Zhang L, Takahashi S, Ma W, Jaffe H, Kulkarni AB, Pant HC. 2002. Cyclin-dependent kinase 5 prevents neuronal apoptosis by negative regulation of c-Jun N-terminal kinase 3. EMBO J 21:324–333.

Mann M, Ong S-E, Gronborg M, Stehn H, Jensen ON, Pandey A. 2002. Analysis of protein phosphorylation using mass spectrometry: Deciphering the phosphoproteom. Trends Biotechnol 6:261–268.

Manning G, Whyte DB, Maritnez R, Hunter T, Sudarsanam S. 2002. The protein kinase complement of the human genome. Science 298:1912–1934.

Muszynska G, Andersson L, Porath J. 1986. Selective adsorption of phosphoproteins on gel-immobilized ferric chelate. Biochemistry 25:6850–6853.

Nelson N. 1993. Presynaptic events involved in neurotransmission. J Physiol 87:171–178.

Nguyen MD, Mushynski WE, Julien J-P. 2002. Cycling at the interface between neurodevelopment and neurodegeneration. Cell Death Differ 9:1294–1306.

Predic J, Soskic V, Bradley D, Godovac-Zimmermann J. 2002. Monitoring of gene expression by functional proteomics: Response of human lung fibroblast cells to stimulation by endothelin-1. Biochemistry 41:1070–1078.

Quest AFG, Soldati T, Hemmer W, Perriard J-C, Eppenberger HM, Wallimann T. 1990. Phosphorylation of chicken brain-type creatine kinase affects a physiologically important kinetic parameter and gives rise to protein microheterogeneity in vivo. FEBS Lett 269:457–464.

Samuels BA, Tsai L-H. 2003. Cdk5 is a dynamo at the synapse. Nat Cell Biol 5:689–690.

Seabra MC, Mules EH, Hume AN. 2002. Rab GTPases, intracellular traffic and disease. Trends Mol Med 8:23–30.

Sharma P, Veeranna D, Sharma M, Amin ND, Shihag RK, Grant P, Ahn N, Kulkarni AB, Pant HC. 2002. Phosphorylation of MEK1 by cdk5/p35 down-regulates the mitogen-activated protein kinase pathway. J Biol Chem 277: 528–534.

Shelton SB, Johnson GVW. 2004. Cyclin-dependent kinase-5 in neurodegeneration. J Neurochem 88:1313–1326.

Shevchenko A, Wilm M, Vorm O, Mann M. 1996. Mass spectrometric sequencing of proteins silver-stained polyacrylamide gels. Anal Chem 68:850–858.

Smith PD, Crocker SJ, Jackson-Lewis V, Jorda-Sciutto KL, Hayley S, Mount MP, O'Hare MJ, Callaghan S, Slack RS, Przedborski S, Anisman H, Park DS. 2003. Cyclin-dependent kinase 5 is a mediator of dopaminergic neuron loss in a mouse model of Parkinson's disease. Proc Natl Acad Sci USA 100:13650–13655.

Sommer S, Hunzinger C, Schillo S, Klemm M, Biefang-Arndt K, Schwall G, Pütter S, Hoelzer K, Schroer K, Stegmann W, Schrattenholz A. 2004. Molecular analysis of homocysteic acid-induced neuronal stress. J Proteome Res 3:572–581.

Soskic V, Görlach M, Poznanovic S, Boehmer FD, Godovac-Zimmermann J. 1999. Functional proteomics analysis of signal transduction pathways of the platelet-derived growth factor beta receptor. Biochemistry 38:1757–1764.

Stanciu M, Wang Y, Kentor R, Burke N, Watkins S, Kree G, Reynolds I, Klann E, Angiolieri MR, Johnson JW, DeFranco DB. 2000. Persistent activation of ERK contributes to glutamate-induced oxidative toxicity in a neuronal cell line and primary cortical neuron cultures. J Biol Chem 275:12200–12206.

Tan TC, Valova VA, Malladi CS, Graham ME, Berven LA, Jupp OJ, Hansra GH, McClure SJ, Sarcevic B, Boadle RA, Larsen MR, Cousin MA, Robinson PJ. 2003. Cdk5 is essentiell for synaptic vesicle endocytosis. Nat Cell Biol 5:701–710.

Walker DH. 1998. Small-molecule inhibitors of cyclin-dependent kinases: Molecular tools and potential therapeutics. Curr Top Microbiol Immunol 227:149–162.

Wang X, Zhu C, Wang X, Gerwien JG, Schrattenholz A, Sandberg M, Leist M, Blomgren K. 2004. The nonerythropoietic asialoerythropoietin protects against neonatal hypoxia-ischemia as potently as erythropoietin. J Neurochem 91:900–910.

Weishaupt JH, Kussmaul L, Grötsch P, Heckel A, Rohde G, Romig H, Bähr M, Gillardon F. 2003. Inhibition of CDK5 is protective in necrotic and apoptotic paradigms of neuronal cell death and prevents mitochondrial dysfunction. Mol Cell Neurosci 24:489–502.

Wüllner U, Seyfried J, Groscurth P, Beinroth S, Winter S, Gleichmann M, Heneka M, Löschmann P-A, Schulz JB, Weller M, Klockgether T. 1999. Glutathione depletion and neuronal cell death: The role of reactive oxygen intermediates and mitochondrial function. Brain Res 826:53–62.

Xia Z, Dickens M, Raingeaud J, Davis RJ, Greenberg ME. 1995. Opposing effects of ERK and JNK-p38 MAP kinases on apoptosis. Science 270:1326–1331.